

# Hematopoietic Islands Mimicking Osteoblastic Metastases in Axial Skeleton

Sophia Samira Goller (✉ [sophia.goller@med.uni-muenchen.de](mailto:sophia.goller@med.uni-muenchen.de))

Ludwig-Maximilians-Universität München

Bernd Erber

Ludwig-Maximilians-Universität München

Nicola Fink

Ludwig-Maximilians-Universität München

Hans Roland Dürr

Ludwig-Maximilians-Universität München

Thomas Knösel

Ludwig-Maximilians-Universität München

Jens Ricke

Ludwig-Maximilians-Universität München

Andrea Baur-Melnyk

Ludwig-Maximilians-Universität München

---

## Research Article

**Keywords:** Hyperplasia of the hematopoietic bone marrow, Hematopoietic islands, Axial skeleton, Osteoblastic metastases, MRI, CT

**Posted Date:** October 11th, 2021

**DOI:** <https://doi.org/10.21203/rs.3.rs-927101/v1>

**License:**  This work is licensed under a Creative Commons Attribution 4.0 International License.

[Read Full License](#)

---

# Abstract

**Background.** Hyperplasia of the hematopoietic bone marrow in the appendicular skeleton is common. Focal hematopoietic islands within the axial skeleton is a rare entity and can cause confusion with osteoblastic metastases. The purpose of this study was to describe the characteristic imaging findings in MRI and CT.

**Methods.** We retrospectively analyzed the imaging findings of 14 hematopoietic islands of the axial skeleton in ten patients (nine females, median age= 65.5 years [range, 49-74]), who received both CT and MRI at the time of initial diagnosis between 2006 and 2020. In five cases CT-guided biopsy was performed to confirm the diagnosis, while the other five patients received long term MRI follow-up (median follow-up= 28 months [range, 6-96 months]). Diffusion-weighted imaging was available in three, chemical shift imaging in two, <sup>18</sup>F fluorodeoxyglucose PET/CT in two and Technetium 99m skeletal scintigraphy in one of the patients.

**Results.** All lesions were small (mean size=1.72 cm<sup>2</sup>) and showed moderate hypointense signals on T1- and T2-weighted MRI sequences. They appeared iso- to slightly hyperintense on STIR images and showed slight enhancement after gadolinium administration. To differentiate this entity from osteoblastic metastases, CT provides important additional information, as hematopoietic islands do not show sclerosis.

**Conclusions.** Hematopoietic islands within the axial skeleton can occur and mimic osteoblastic metastases. However, the combination of MRI and CT allows for making the correct diagnosis.

## 1. Background

While bone marrow in the fetus is entirely hematopoietic, conversion to fatty marrow begins in the distal extremities soon after birth and is confined to the axial skeleton, proximal humeri, femoral neck, and intertrochanteric regions by young adulthood. The haematopoietic marrow itself is composed of cellular components and varying amounts of fat, whereby the fat content increases with age (1).

Mild forms of hyperplasia of the red bone marrow are associated with heavy smoking, long distance running, and obesity (2-4). More severe and diffuse forms can be found in association with chronic anemias (in particular hemolytic types) and both benign and malignant infiltrative bone marrow disorders, such as Gaucher disease, myelofibrosis, myeloma, lymphoma, leukemia and metastatic disease (2, 5, 6). In cancer patients, hematopoietic marrow hyperplasia can be encountered as well after the administration of granulocyte-colony-stimulating factors (7, 8).

Since peripheral manifestations of hematopoietic bone marrow hyperplasia are significantly more common than those of the axial skeleton, these foci are often accidentally seen on routine MRI of the lower extremities, in particular around the knee joint, as previously described in a case series of Deutsch et al. (2). However, focal hyperplasia of the red marrow has been found within the axial skeleton as well,

which was described in a case report by Bordalo-Rodrigues et al. in 2002 (9). In addition, two previous case reports reported the detection of focal hematopoietic hyperplasia in the ribs (10, 11).

Diagnostic difficulties may arise in distinguishing focal hematopoietic hyperplasia of the axial skeleton (“hematopoietic islands”) from osteoblastic vertebral metastases, particularly when an underlying malignancy is known.

Therefore, the purpose of our study was to evaluate and characterize typical MRI and CT findings of hematopoietic islands of the axial skeleton to help both radiologists and clinicians on the one hand not to overdiagnose this entity and on the other hand to decide on a reasonable work-up. Newer imaging techniques, such as diffusion-weighted (DWI), chemical shift and hybrid imaging techniques were evaluated in a subgroup of our patients.

## **2. Methods**

### **2.1 Patient population**

This retrospective single-center analysis included ten patients with 14 hematopoietic islands of the axial skeleton who underwent both MRI and CT at the time of initial diagnosis between January 2006 and January 2020 (patient characteristics are summarized in Table 1). In detail, patients were retrospectively identified via a full text query within the local radiology information system using the term “hematopoietic island”. Subsequently, the resulting reports were further filtered with respect to the availability of initial MRI and CT examinations and to the presence of sufficiently long follow-up periods (at least 6 months) and/or histologically confirmed lesions. In two patients despite biopsy-confirmed diagnosis, long-term follow-up of 28 respectively 50 months was available.

Table 1  
Patient characteristics

	Age	Sex	Lesion localisation [n]	Lesion size*	Previous malignancy	Primary CT-guided biopsy	MRI follow-up [months]
1	66	f	Thoracic spine [3] Lumbar spine [1]	0,8 x 0,6 1,0 x 1,0 1,6 x 1,2 1,6 x 1,6	Breast cancer	yes	28**
2	67	f	Os sacrum [1]	1,3 x 1,1	Gastric SRCC	no	96
3	64	f	Os sacrum [1]	1,1 x 1,2	Breast cancer	yes	
4	65	f	Os sacrum [1]	1,6 x 1,7	no	yes	
5	53	f	Rib [1]	1,8 x 0,8	no	yes	50**
6	50	f	Lumbar spine [1]	1,5 x 1,3	Breast cancer (IDC)	no	29
7	73	f	Lumbar spine [1]	1,0 x 0,9	no	no	20
8	72	f	Thoracic spine [1]	1,3 x 1,2	no	no	6
9	49	m	Lumbar spine [1] Os ilium [1]	1,0 x 1,0 1,2 x 1,3	no	yes	
10	74	f	Lumbar spine [1]	2,1 x 1,8	no	no	11

f, female; m, male; SRCC, signet ring cell carcinoma; IDC, invasive ductal carcinoma

\*lesion size [cm x cm, axial T2 weighted MRI images]

\*\*additional MRI follow-up in case of primary CT-guided biopsy

	Age	Sex	Lesion localisation [n]	Lesion size*	Previous malignancy	Primary CT-guided biopsy	MRI follow-up [months]
<b>Total [n]</b>	<b>Mean [years]</b>	<b>Male/female ratio [n]</b>	<b>Total [n]</b>	<b>Mean [cm<sup>2</sup>]</b>	<b>Total [n]</b>	<b>Total [n]</b>	<b>Mean [months]</b>
10	63.3 (49-74)	1/9	14	1.72 (0.48-3.78)	4	5	34.2 (6-96)
	<b>Median [years]</b>			<b>Median [cm<sup>2</sup>]</b>			<b>Median [months]</b>
	65.5			1.46			28
f, female; m, male; SRCC, signet ring cell carcinoma; IDC, invasive ductal carcinoma							
*lesion size [cm x cm, axial T2 weighted MRI images]							
**additional MRI follow-up in case of primary CT-guided biopsy							

## 2.2 Imaging

All MRI examinations were conducted using 1.5 Tesla MRI (Avanto, Siemens Healthineers, Erlangen, Germany). MRI protocols routinely comprised the following sequences: T1-weighted (T1w) turbo spin-echo (TSE) sequences, T2-weighted TSE sequences, and short-tau inversion recovery (STIR) sequences, each with a slice thickness of 3-4 mm. Gadolinium-enhanced T1-weighted sequences were acquired in nine of the ten patients. Diffusion-weighted imaging (DWI) using a reverse fast imaging with steady-state free precession sequence (SSFP) was done in three, and chemical shift imaging in two of the patients.

All patients underwent high-resolution CT at least once at the time of initial diagnosis. Two of the patients received complementary <sup>18</sup>F fluorodeoxyglucose (FDG) PET/CT and one Technetium (Tc) 99m skeletal scintigraphy.

We analyzed the location and size (maximum diameter on either axial or sagittal images) as well as the signal intensities on all standard morphological MRI sequences (T1 TSE, T2 TSE, STIR, T1 post contrast). We evaluated bone texture changes (osteosclerosis/-lysis) on CT scans, as well as FDG-uptake on PET-CT in two cases and radiotracer accumulation on skeletal scintigraphy in one case. In addition, signal behavior on DWI and chemical shift imaging was analyzed according to the known methods (12). Using SSFP sequences, the signal intensity of each lesion was assessed qualitatively in relation to adjacent bone marrow as hypo-, iso- or hyperintense. According to Zajick et al. decreases in signal intensity greater than 20% on out-of-phase images compared with in-phase images have been used as a cut-off threshold for normalcy to allow distinction between benign (>20% signal decrease on out-of-phase images) and malignant (<20% signal decrease on out-of-phase images) marrow changes on chemical shift imaging (13).

### 3. Results

A total of 14 lesions in ten patients could be found. One patient showed four lesions, while all of the other patients presented with one single lesion. The lesions were located at the thoracic spine (n= 4), lumbar spine (n=5), Os sacrum (n=3), Os ilium (n=1) and at the rib (n=1). Lesion size ranged from 0.48-3.78 cm<sup>2</sup> (mean: 1.72 cm<sup>2</sup>). All lesions had fairly sharp margins and were well demarcated from adjacent bone marrow. Detailed patients and lesions characteristics are summarized in Table 1, typical imaging findings in Table 2.

### 3.1 MRI

Without exception, all lesions presented moderate hypointense signals on T1w and T2w imaging (n=14) (Fig. 1a, b, Fig. 2a, b), while being iso- (n=5) to slightly hyperintense on STIR-sequences (n=9) (Fig. 1c, Fig. 2c).

After gadolinium- administration, all lesions (n=13) showed mild enhancement (Fig. 1d, Fig. 2d). In n=3 patients DWI with a SSFP sequences was performed, where all lesions presented hypointensity in comparison to adjacent normal bone marrow (Fig. 2e). On chemical shift imaging (n=2) lesions showed a signal drop of greater than 20% on out-of-phase images compared with in-phase images, indicating fat within the lesions.

### 3.2 CT

None of the hematopoietic islands showed abnormalities of the bone structure in terms of sclerotic or lytic changes on CT (Fig. 1e, Fig. 2f).

Table 2  
Characteristic imaging findings of hematopoietic islands in contrast to osteoblastic metastases on MRI and CT

Imaging	Hematopoietic islands	Osteoblastic metastases
T1w	Slightly hypointense	Markedly hypointense
T2w	Slightly hypointense	Markedly hypointense
STIR	Iso- slightly hyperintense	Iso- hypointense
ce T1w	Slight enhancement	No/slight enhancement
CT	No sclerotic or lytic bone changes	Sclerosis

*w, weighted; STIR, short-tau inversion recovery; ce, contrast-enhanced (gadolinium)*

### 3.3 PET-CT

In n=2 patients, who received complementary  $^{18}\text{F}$  FDG PET/CT, FDG-uptake was not increased (cut-off value  $\text{SUV}_{\text{max}} > 3$  considered pathologic).

## 3.4 Skeletal scintigraphy

Tc 99m skeletal scintigraphy was unremarkable in n=1 patient.

## 4. Discussion

We presented characteristic MRI and CT findings of hematopoietic islands of the axial skeleton in a case series of ten patients. The awareness of this rare entity is important in order not to misdiagnose these lesions as osteoblastic metastases, which typically show similar signal intensities on MRI. Diagnostic difficulties particularly arise when an underlying malignancy is known.

### MRI

Normal bone marrow shows intermediate signal intensity on T1w spin-echo images since it contains about 50% fat and 50% water in adults (14). In our patient cohort, all hematopoietic islands presented moderate hypointense signal on unenhanced T1w TSE MR images compared to surrounding marrow. This is explained by the fact that in hematopoietic islands a marked amount of fat is still preserved. Our finding is consistent with previous reported cases of focal hematopoietic islands (2, 9-11). They were also mild hypointense on T1w TSE images, which is helpful in differentiating these lesions from osteoblastic metastases, which usually show strong T1w signal drop iso- or hypointense compared to adjacent muscle or disk (15, 16).

Unenhanced T1w sequences are important in differentiating benign lesions with fat content (like benign bone marrow lesions or edema) from metastases, which normally show a significant reduction in fat component due to cellular replacement with marrow infiltration (17). In a previous study, Carroll et al. analyzed T1w images of 74 patients with both benign and malignant bone marrow signal alterations on MRI (51 biopsy-proven, 23 clinical follow-up) and compared relative signal intensity of bone marrow to adjacent skeletal muscle and/or nondegenerated intervertebral disk in order to establish standards on MRI differentiating infiltrative marrow pathology from hematopoietic marrow. It was summarized that marrow lesions that are relatively isointense or hypointense to muscle and/or disk on T1w spin-echo images should not be considered normal hematopoietic marrow (15).

Schweitzer et al. previously reported the “bull’s eye sign” as a specific indicator of normal hematopoietic marrow and the “halo sign” as a strong indicator of metastatic disease in 47 patients with osseous lesions of the pelvis evaluating T1w and T2w sequences (18). The “bull’s eye sign”, which describes a central T1w high signal intensity in an osseous lesion, could not be found in our cases of hematopoietic islands. Thus, T1w TSE images are important for the differentiation of sclerotic osteoblastic metastases with strong hypointense signal equal to adjacent disc or muscle and focal hematopoietic islands with only moderate signal drop.

Normal bone marrow shows intermediate signal intensity on T2w TSE images. In our cohort, all hematopoietic islands showed hypointense signals on T2w TSE images, which is similar to osteoblastic metastases. In contrast, osteolytic metastases show high signal intensity on T2w images (14, 19, 20). All previous reported hematopoietic islands as well showed hypointense T2w signals, which is in concordance with our findings (2, 9-11).

STIR sequences provide high tissue contrast by suppressing fat signals. Thus, all pathologic processes, such as metastases, edema, and inflammation show strong hyperintense signals. Normal bone marrow usually shows low signal intensity on STIR imaging (14, 20). Five out of 14 lesions in our cohort showed isointense signals on STIR sequences compared to adjacent bone marrow, while nine showed slightly hyperintense signals. In contrast, osteolytic metastases typically show strong hyperintense signals on STIR sequences, while osteoblastic metastases show similar signal behavior to hematopoietic islands due to a lack of water protons (14).

Thus, T2w TSE and STIR imaging are not helpful in differentiating focal hematopoietic islands from osteoblastic metastases.

After gadolinium administration normal bone marrow enhances to a certain extent (21). Osteoblastic metastases typically show also no or only slight enhancement, while osteolytic lesions strongly enhance (14, 19, 20). Hematopoietic islands in our cohort showed slight enhancement after contrast administration, which was more conspicuous on fat-saturated images. Thus, gadolinium cannot differentiate between osteoblastic metastases and focal hematopoietic islands but are helpful in differentiating them from osteolytic or mixed type metastases, which usually show strong enhancement. As of yet, there are no previous studies describing the signal behavior of hematopoietic islands after gadolinium administration. In general in uncertain bony lesions, contrast administration is highly recommended (22).

### Diffusion-weighted imaging

DWI is based on quantifying the motion of water molecules within tissue (23). Three patients of our cohort received DWI with obtaining SSFP sequences with relatively short acquisition time and insensitivity for patient movement. All examined hematopoietic islands presented as hypointense lesions when qualitatively compared to adjacent bone marrow. In previous studies, SSFP imaging was able to differentiate between malignant, depicted as hyperintense, and benign vertebral fractures, depicted as iso- or hypointense in comparison to normal bone marrow (23, 24). However, osteoblastic metastases may also present hypointensity on SSFP sequences due to sclerosis (25, 26). Thus, DWI is not of definite value in distinguishing these two entities.

### Chemical Shift- imaging

Chemical shift imaging, which can be used to quantitatively assess the fat and water content of vertebral bone marrow on a voxel-by-voxel-basis, was done in two patients in our cohort (12). In a previous study of

Zajick et al. on 221 marrow lesions in 92 patients a signal drop of more than 20% on out-of-phase images compared with in-phase images indicated benign lesions (13). In accordance with benign lesions, all hematopoietic islands in our patient cohort showed signal drops greater than this 20% threshold on out-of-phase images due to their fat content. In contrast, in malignant lesions normal fat-containing marrow is replaced with high cellular tumorous tissue, which has the effect that this increase in water protons is associated with a lack of suppression on the out-of-phase images (13, 27, 28). Thus, chemical shift imaging seems to be of value for the differentiation of hematopoietic islands of the axial skeleton and osteoblastic metastases.

### CT Imaging

On CT none of the lesions showed sclerosis, which is in contrast to osteoblastic metastases. This is a strong and important imaging feature to make the correct diagnosis.

### Hybrid Imaging Techniques

<sup>18</sup>F FDG PET-CT was done in two patients. No increased FDG uptake was found in both patients (cut-off value  $SUV_{max} > 3$ ). This is in contrast to a previous case report of Bordalo-Rodrigues et al. He reported a case of a patient with lung carcinoma, who received <sup>18</sup>F FDG PET-CT examination as pretherapeutic staging, where increased uptake was noted in a biopsy-proven hematopoietic island in the vertebral body of Th8 (9). Taking these findings into account, it has to be stated that focal areas of normal but hypercellular red marrow may show increased uptake on FDG PET-CT and therefore may be confused with neoplasm or infection. This may be due to upregulation of glucose transporters and metabolism in stimulated cells, also known from increased FDG-uptake in patients undergoing treatment with granulocyte-colony-stimulating-factor, which stimulated growth and differentiation of hematopoietic stem cells. However, in these cases- in contrast to hematopoietic islands- FDG-uptake is diffuse (7, 8).

Possibly, the hematopoietic activity in our lesions might have been too low to cause an increased FDG-uptake. It should be emphasized that hematopoietic islands may remain occult on FDG PET-CT. Therefore, FDG PET-CT is not of direct value for the differentiation of osteoblastic metastases and focal hematopoietic islands of the spine.

### Skeletal scintigraphy

Tc 99m skeletal scintigraphy was performed in one patient in our cohort and was unremarkable. This is in contrast to a previous report of Lee et al., who described an increased radiotracer accumulation in a focal hematopoietic hyperplasia of the right third rib in a 24-year-old patient (11). Thus, skeletal scintigraphy is not of value in distinguishing hematopoietic islands from osteoblastic metastases.

### Bone marrow biopsy

Five patients received CT-guided biopsy in order to confirm the diagnosis. All samples showed proportions of bone marrow with moderately increased hematopoiesis. The fat cell content was mildly

reduced. There was no evidence of malignancy (Fig. 1f, Fig. 2g).

## Limitations

A limitation of our study is the small number of patients. However, so far, there is little literature available on this topic. In addition, biopsy was obtained in only five patients, however osteoblastic metastases could be excluded by CT and follow-up MRI. Furthermore, not all patients received DWI, chemical shift and hybrid imaging. However, typical routine sequences (T1w TSE, T2w TSE and STIR) were available in all of the patients. In addition, gadolinium was applied in nine out of ten patients.

## 5. Conclusions

Hematopoietic islands of the axial skeleton are a rare entity and may easily be confused with osteoblastic metastases, due to similar signaling behavior on standard morphological MRI. A hint to make the diagnosis of hematopoietic islands versus osteoblastic metastases is the only moderate signal reduction on unenhanced T1w images typically seen in this rare entity. Therefore, we highly recommend performing MRI in combination with CT at initial diagnosis, since osteoblastic metastases are characterized by sclerosis. Thus, this major differential diagnosis can be excluded. Chemical shift imaging seems to be of value in demonstrating the fat content in focal hematopoietic islands in contrast to osteoblastic metastases. In unclear cases, early histologic confirmation of the bone marrow lesion e.g., via CT-guided biopsy, is reasonable, particularly in tumor patients.

## Abbreviations

<sup>18</sup>F-FDG-PET-CT: <sup>18</sup>F-fluorodeoxyglucose Positron Emission Tomography; Tc-99m: Technetium 99m; CT: Computed Tomography; DWI: Diffusion-weighted imaging; MRI: Magnetic resonance imaging; SSFP: Steady-State Free Precession; STIR: Short-Tau Inversion Recovery; TSE: Turbo spin-echo; T1w: T1-weighted; T2w: T2-weighted

## Declarations

### Ethics approval and consent to participate

This study was approved by the ethics committee of the Medical Faculty, University of Munich (project number 21-0124). Written consent was obtained from all patients included in this study. The study was conducted according to the Declaration of Helsinki of 1964 and its later amendments.

### Consent for publication

All patients included in this study gave consent for publishing their clinical details along with any radiological images to be published in this study.

### Availability of data and materials

The datasets analysed during the current study are available from the corresponding author on reasonable request.

### **Competing interests**

The authors declare that they have no competing interests.

### **Funding**

This research did not receive any specific grant from funding agencies in the public, commercial, or not-for-profit sectors.

### **Authors' contributions**

SG. Corresponding author. Developed the study concept, did the data analysis and provided the major input in writing and revising the manuscript. BE and NF. Radiology residents helped with data collection and image analysis. HRD. Orthopaedic surgeon on many of the cases. TK. Pathologist analyzing the histopathological investigations. JR. Senior radiologist reviewing the study conceptualization and data analysis. ABM. Senior radiologist reviewing the radiological investigations and revising the manuscript. Each author made substantial contributions to study conception and design or acquisition of data and data analysis. All authors have been involved in the drafting and critical revision of the manuscript. All authors read and approved the final version of the manuscript.

### **Acknowledgements**

Not applicable.

## **References**

1. Mitchell DG, Rao VM, Dalinka M, Spritzer CE, Axel L, Gefter W, et al. Hematopoietic and fatty bone marrow distribution in the normal and ischemic hip: new observations with 1.5-T MR imaging. *Radiology*. 1986;161(1):199–202.
2. Deutsch AL, Mink JH, Rosenfelt FP, Waxman AD. Incidental detection of hematopoietic hyperplasia on routine knee MR imaging. *AJR Am J Roentgenol*. 1989;152(2):333–6.
3. Poulton TB, Murphy WD, Duerk JL, Chapek CC, Feiglin DH. Bone marrow reconversion in adults who are smokers: MR Imaging findings. *AJR Am J Roentgenol*. 1993;161(6):1217–21.
4. Shellock FG, Morris E, Deutsch AL, Mink JH, Kerr R, Boden SD. Hematopoietic bone marrow hyperplasia: high prevalence on MR images of the knee in asymptomatic marathon runners. *AJR Am J Roentgenol*. 1992;158(2):335–8.
5. Stabler A, Doma AB, Baur A, Kruger A, Reiser MF. Reactive bone marrow changes in infectious spondylitis: quantitative assessment with MR imaging. *Radiology*. 2000;217(3):863–8.

6. Kricun ME. Red-yellow marrow conversion: its effect on the location of some solitary bone lesions. *Skeletal Radiol.* 1985;14(1):10–9.
7. Hollinger EF, Alibazoglu H, Ali A, Green A, Lamonica G. Hematopoietic cytokine-mediated FDG uptake simulates the appearance of diffuse metastatic disease on whole-body PET imaging. *Clin Nucl Med.* 1998;23(2):93–8.
8. Yao WJ, Hoh CK, Hawkins RA, Glaspy JA, Weil JA, Lee SJ, et al. Quantitative PET imaging of bone marrow glucose metabolic response to hematopoietic cytokines. *J Nucl Med.* 1995;36(5):794–9.
9. Bordalo-Rodrigues M, Galant C, Lonneux M, Clause D, Vande Berg BC. Focal nodular hyperplasia of the hematopoietic marrow simulating vertebral metastasis on FDG positron emission tomography. *AJR Am J Roentgenol.* 2003;180(3):669–71.
10. Edelstein G, Kyriakos M. Focal hematopoietic hyperplasia of the rib—a form of pseudotumor. *Skeletal Radiol.* 1984;11(2):108–18.
11. Lee KB, Kim BS, Cho JH. Focal hematopoietic hyperplasia of the rib. *Skeletal Radiol.* 2002;31(3):175–8.
12. Schwaiger BJ, Gersing AS, Baum T, Krestan CR, Kirschke JS. Distinguishing Benign and Malignant Vertebral Fractures Using CT and MRI. *Semin Musculoskelet Radiol.* 2016;20(4):345–52.
13. Zajick DC, Jr., Morrison WB, Schweitzer ME, Parellada JA, Carrino JA. Benign and malignant processes: normal values and differentiation with chemical shift MR imaging in vertebral marrow. *Radiology.* 2005;237(2):590–6.
14. Shah LM, Hanrahan CJ. MRI of spinal bone marrow: part I, techniques and normal age-related appearances. *AJR Am J Roentgenol.* 2011;197(6):1298–308.
15. Carroll KW, Feller JF, Tirman PF. Useful internal standards for distinguishing infiltrative marrow pathology from hematopoietic marrow at MRI. *J Magn Reson Imaging.* 1997;7(2):394–8.
16. Zhao J, Krug R, Xu D, Lu Y, Link TM. MRI of the spine: image quality and normal-neoplastic bone marrow contrast at 3 T versus 1.5 T. *AJR Am J Roentgenol.* 2009;192(4):873–80.
17. Vande Berg BC, Malghem J, Lecouvet FE, Maldague B. Classification and detection of bone marrow lesions with magnetic resonance imaging. *Skeletal Radiol.* 1998;27(10):529–45.
18. Schweitzer ME, Levine C, Mitchell DG, Gannon FH, Gomella LG. Bull's-eyes and halos: useful MR discriminators of osseous metastases. *Radiology.* 1993;188(1):249–52.
19. Vande Berg BC, Malghem J, Lecouvet FE, Maldague B. Magnetic resonance imaging of normal bone marrow. *Eur Radiol.* 1998;8(8):1327–34.
20. Vogler JB, 3rd, Murphy WA. Bone marrow imaging. *Radiology.* 1988;168(3):679–93.
21. Baur A, Stabler A, Bartl R, Lamerz R, Scheidler J, Reiser M. MRI gadolinium enhancement of bone marrow: age-related changes in normals and in diffuse neoplastic infiltration. *Skeletal Radiol.* 1997;26(7):414–8.
22. Georgy BA, Hesselink JR, Middleton MS. Fat-suppression contrast-enhanced MRI in the failed back surgery syndrome: a prospective study. *Neuroradiology.* 1995;37(1):51–7.

23. Baur A, Stabler A, Bruning R, Bartl R, Krodel A, Reiser M, et al. Diffusion-weighted MR imaging of bone marrow: differentiation of benign versus pathologic compression fractures. *Radiology*. 1998;207(2):349–56.
24. Geith T, Schmidt G, Biffar A, Dietrich O, Durr HR, Reiser M, et al. Comparison of qualitative and quantitative evaluation of diffusion-weighted MRI and chemical-shift imaging in the differentiation of benign and malignant vertebral body fractures. *AJR Am J Roentgenol*. 2012;199(5):1083–92.
25. Castillo M, Arbelaez A, Smith JK, Fisher LL. Diffusion-weighted MR imaging offers no advantage over routine noncontrast MR imaging in the detection of vertebral metastases. *AJNR Am J Neuroradiol*. 2000;21(5):948–53.
26. Hacklander T, Scharwachter C, Golz R, Mertens H. [Value of diffusion-weighted imaging for diagnosing vertebral metastases due to prostate cancer in comparison to other primary tumors]. *Rofo*. 2006;178(4):416–24.
27. Eryl WK, Oh ES, Outwater EK. The utility of in-phase/opposed-phase imaging in differentiating malignancy from acute benign compression fractures of the spine. *AJNR Am J Neuroradiol*. 2006;27(6):1183–8.
28. Ragab Y, Emad Y, Gheita T, Mansour M, Abou-Zeid A, Ferrari S, et al. Differentiation of osteoporotic and neoplastic vertebral fractures by chemical shift {in-phase and out-of phase} MR imaging. *Eur J Radiol*. 2009;72(1):125–33.

## Figures

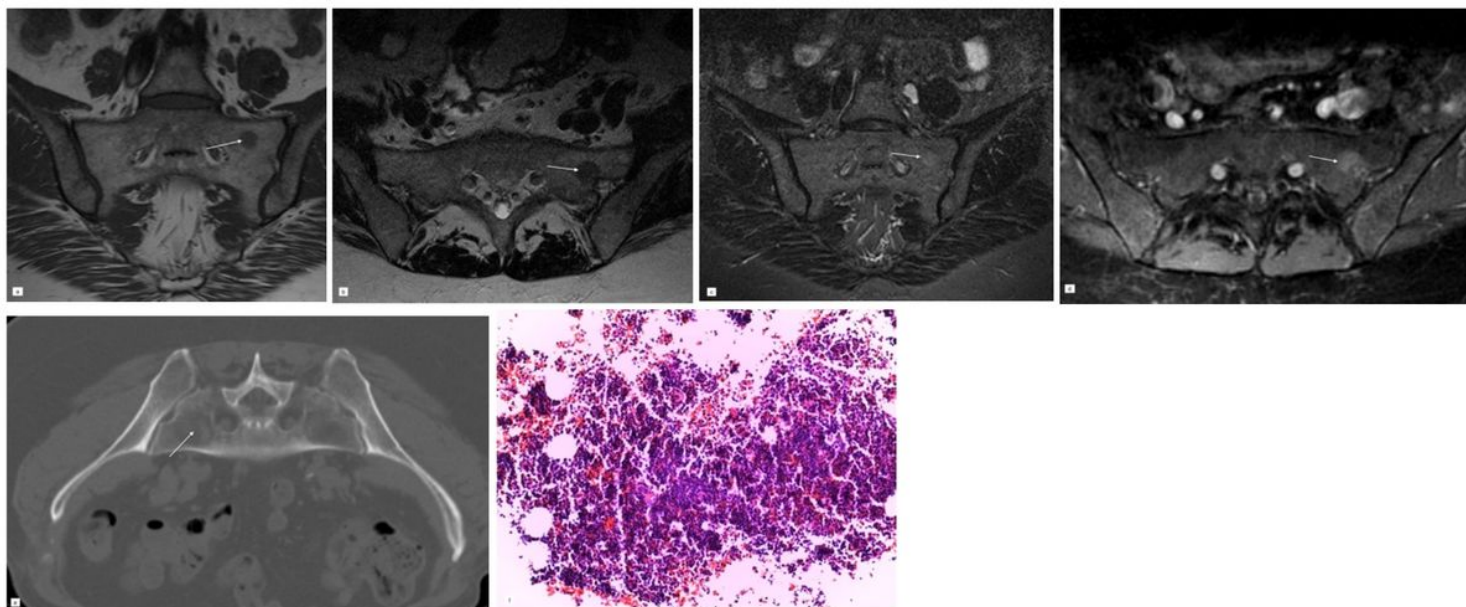


**Figure 1**

64-year-old woman with history of breast cancer and focal hyperplasia of hematopoietic marrow in sacral spine (S1)\* \*arrows point to the S1 lesion; H&E, hematoxylin and eosin a: Coronal T1w TSE MR image of

sacral spine shows focal area of moderately decreased signal intensity in vertebral body of S1. b: Axial T2w TSE image with (corresponding to a) signal drop in S1. c: Slight hyperintense signal of S1 lesion is shown on coronal STIR image. d: On axial contrast enhanced fat-saturated T1w image S1 lesion shows slight enhancement. e: High-resolution CT scan (note: prone position before CT-guided biopsy was performed) without any bone structure abnormalities in S1. f: Photograph of biopsy specimen (H&E, x80) of S1 lesion shows hypercellular bone marrow with reduced number of adipocytes. No neoplastic cells were found.



**Figure 2**

66-year-old woman with history of breast cancer and focal hyperplasia of hematopoietic marrow in thoracic (Th10, 11, 12) and lumbar spine (L1)\* \*images illustrating Th12 and L1 lesions (arrows); SSFP, fast imaging with steady-state precession sequence; H&E, hematoxylin and eosin a: Sagittal T1w TSE MR image of thoracic and lumbar spine shows focal area of moderately decreased signal intensity in vertebral bodies of Th12 and L1. b: Sagittal T2w TSE image with signal drop in Th12 and L1 (corresponding to a). c: Sagittal STIR image with slightly hyperintense signal in Th12 and L1 lesions. d: Lesions show slight focal enhancement after administration of gadolinium on sagittal T1w image. e: Sagittal SSFP image with hypointense signal of both Th12 and L1 lesion. f: High-resolution CT scan without any bone structure abnormalities in Th12 and L1. g: Photograph of biopsy specimen (H&E, x80) of Th12 lesion shows hypercellular bone marrow with reduced portion of adipocytes.